Compact High-Isolation Multiplexer With Wide Stopband Using Spiral Defected Ground Resonator

KAIJUN SONG, (Senior Member, IEEE), **YEDI ZHOU**, **YUXUAN CHEN**,
SHEMA RICHARD PATIENCE, **SONG GUO**, (Student Member, IEEE),
AND YONG FAN, (Senior Member, IEEE)

EHF Key Laboratory of Science, School of Electronic Science and Engineering, University of Electronic Science and Technology of China, Chengdu 611731, China

Corresponding author: Kaijun Song (ksong@uestc.edu.cn)

ABSTRACT In this paper, the compact wide-stopband diplexer/triplexer is presented. The spiral defected ground resonator (SDGR) is analyzed by using the equivalent model. Based on the symmetry of the SDGR, a diplexer and a triplexer are implemented with a miniaturized size and a wide stopband. Each filter of the channels in the diplexer or triplexer can be independently controlled and exhibits a constant fractional bandwidth. To validate the design concept, the diplexer and the triplexer are designed, fabricated, and measured. The isolation between the channels is greater than 30 dB, and the measured out-of-band suppression is greater than 10 dB in the very wide frequency range. The measured results agree well with the simulation ones.

INDEX TERMS Diplexer, triplexer, spiral defected ground resonator (SDGR), compact, wide stopband.

I. INTRODUCTION

With the rapid development of industrial electronics, various radio frequency (RF) circuits/devices have been presented and studied [1]–[12]. In order to meet the requirements of the system miniaturization, the compact microwave devices are being quickly put forward [2], [13]–[18]. As key devices in modern wireless systems of industrial electronics, the diplexer /multiplexer [1], [17], in separation mode, can separate one wideband input signal into many narrowband output signals. Therefore, the diplexer/multiplexer have been studied by more and more scholars. The microstrip-line diplexer/multiplexer has the advantage of low cost, easy fabrication, and can process various planar shapes [1], [19].

Since the multiplexer is a synthesis of the filter group, the adjacent filters interact with each other. The in-band characteristic of a single filter is deteriorated, which increases the difficulty of the multiplexer design and optimization. In the design process of diplexer, there are two main methods of miniaturization. One method is the application of a step impedance resonators (SIRs) [21], and the other is the

introduction of a multimode resonator [22]–[25]. In addition, the ground defective structure, embedded electromagnetic band gap, artificial electromagnetic metamaterials can also make the diplexer miniaturization. SIR not only can control independently the harmonics, but also can reduce the size of the resonator. In [28], the SIR has been used to suppress spurious frequency. In [29], the substrate-integrated rectangular cavity (SIRC) resonator, similar to the SIR, was analyzed and a filter with the wide-stopband response was obtained by designing resonators with different modes. However, the circuit size of SIR or SIRC is still large.

The application of multimode resonators is also an important way to design diplexers/multiplexers. The channel filter is coupled to a common resonator with multiple resonant modes, and the diplexer is obtained by controlling the resonant mode. The introduction of the common resonator makes the design of the matching network omitted, simplifying the circuit design. A diplexer is designed with T-type dual-mode resonator in [19]. Using the resonant characteristics of the T-type dual-mode resonator, two resonant frequencies of the dual-mode resonator are set to the center frequencies of the two passbands of the diplexer. High isolation of the two channels is achieved. Similarly, a triplexer is designed using a

---

The associate editor coordinating the review of this manuscript and approving it for publication was Xiu Yin Zhang.

tri-mode resonator as a common resonator in [30]. However, the multiplexer with more filter channels is difficult to use this structure to achieve. Since the resonant mode of the common resonator is limited, the center frequency of each passband cannot be independently adjusted. This adds difficulty to the analysis and design of the circuit.

The concept of Defected Ground Structure (DGS), which is realized by etching a few defects on the ground plane under the microstrip line, was presented in [31] and [32]. An etched lattice shape is proposed as a DGS unit cell. The circuit characteristics and their circuit equivalent models are given when the feedline is not separated. It provides good bandgap and slow-wave effects by slotting on the ground such as PBG and is applied to low pass filters and bandpass filters [33]–[35] without taking up extra space. Reference [36] presents a defective step impedance resonator and is used to design a compact quadruplexer. The relative position of the separated coupling feedline is reasonably placed, and the influence of the adjacent channel is weakened. Multiple channel matching can be achieved without the need for redundant matching networks, providing great flexibility for diplexer/multiplexer design.

A spiral-shipped DGS has been presented in [37] and [38] for coplanar wave guide and microstrip line respectively. Compared to dumbbell-shape DGS, DGS can provide higher slow wave characteristics, which means that it has the potential for higher frequencies, and more compact features.

In this paper, in order to achieve miniaturization, high isolation and wide stopband, the multiplexer based on spiral resonators is designed in section II. Its equivalent circuit is given, providing the basis for the filter design. Compact diplexer with high isolation and wide stopband are developed. Due to the use of separate feedline coupling technology, the matching network is simplified and the circuit size is further reduced. In section III, a compact triplexer is designed to further validate the feasibility of DGS. The measured results are in good agreement with the simulation ones.

II. STRUCTURE AND DESIGN OF THE DIPLEXER
A. DESIGN AND ANALYSIS OF THE SDGR

shows the structure of the spiral defected ground resonator (SDGR). The SDGR is composed of two feedlines and a rectangular spiral, etched on the metal ground. The microwave signal is transmitted to the SDGR by feedline through the edge coupling. According to Fig.1 (a) and (b), it can be found that the central frequency is correlated to l_0. The change of coverage length (l_c) will lead to the change of energy coupling, as shown in Fig. 1(b), then the resonant frequency of the resonator will change.

Fig. 2 shows the resonant frequency and magnitude. The SDGR has a self-resonant frequency, which results in a finite-frequency attenuation pole in the upper stopband. In addition, it can be seen that the resonant frequency increases high with the decreasing l_0.
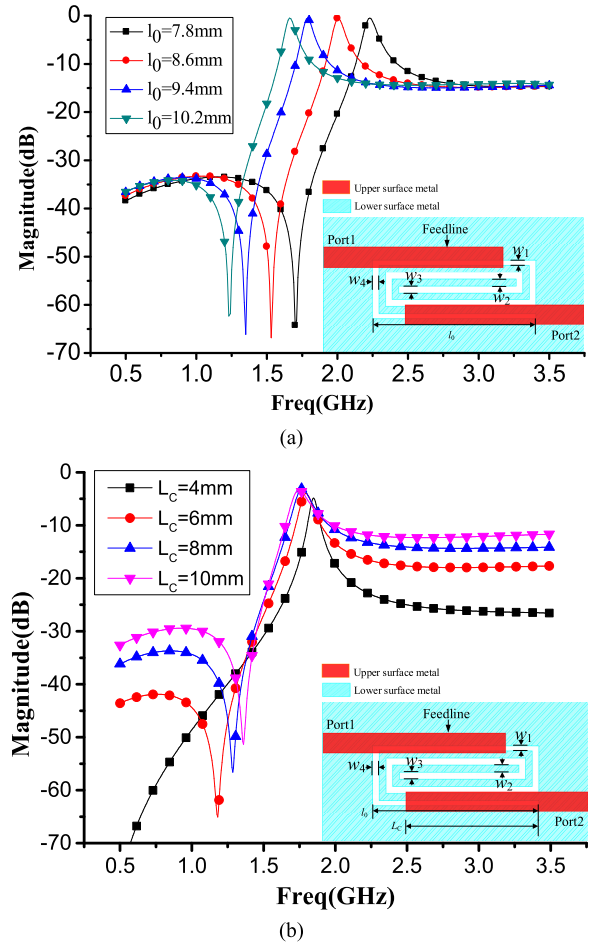

FIGURE 1. Structure of the SDGR(with fixed $w1 = w2 = w3 = w4 = 0.2$mm). (a) simulated results of the SDGR versus l_0. (b) simulated results of the SDGR versus L_C.
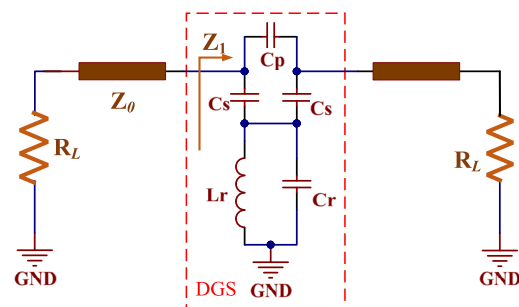

FIGURE 2. Equivalent circuit of the proposed SDGR.

The SDGR can be analyzed by the equivalent circuit method. As shown in Fig. 2, the 50 ohm transmission line can be equivalent to series inductors and capacitors. The capacitor C_p represents the coupling between feedlines. Similarly, spiral structure etched on the metal floor is equivalent a parallel LC circuit which consist of L_r and C_r. In addition, the coupling between the feedline and the resonator is equivalent by capacitance C_s.
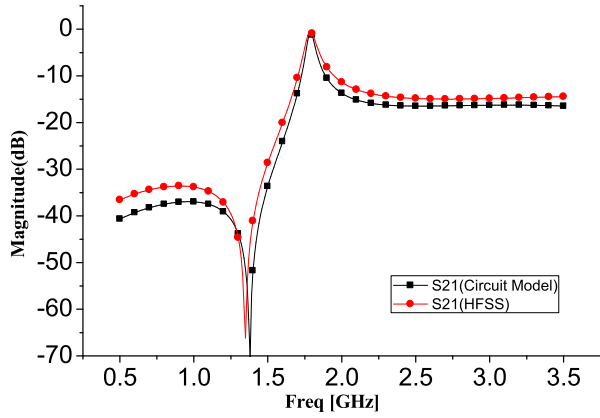
FIGURE 3. Comparisons between the HFSS full wave simulation result and circuit model.

As shown in Fig. 2, the equivalent impedance when other port opened can be get

$$Z_1 = \frac{j \left[\omega^2 L_r \left(C_r + C_s' \right) - 1 \right]}{\omega C_s' \left(1 - \omega^2 L_r C_r \right)} \tag{1}$$

where C_s' is obtained by the equivalent of the Cs and Cp circuit networks.

Further, the positions of the transmission zero f_z and the transmission pole f_0 are respectively obtained as follows

$$f_z = \frac{1}{2\pi \sqrt{L_r \left(C_r + C_s' \right)}} \tag{2}$$

$$f_0 = \frac{1}{2\pi \sqrt{L_r C_r}} \tag{3}$$

When the feedline is not separated, the DGS transmission is represented by bandgap characteristics. The circuit model is equivalent to a parallel resonant network. The center frequency is the same as the transmission pole f_0, and the equivalent parallel inductance L_r and C_r is consistent. Thus, the present equivalent model parameters of the SDGR can be calculated [39]

$$R = 2Z_0(1/ |S_{21}| - 1)|_{f=f_0} \tag{4}$$

$$C_r = \frac{\sqrt{0.5 \left(R + 2Z_0 \right)^2 - 4Z_0^2}}{2.83\pi Z_0 R \Delta f} \tag{5}$$

$$L_r = 1/4 \left(\pi f_0 \right)^2 C_r \tag{6}$$

where Z_0 is the characteristic impedance of the transmission, S_{21} is the insertion loss, which is measured when the feeder is not separated [39]. Δf is the 3 dB bandwidth. The comparison between the simulation results and the circuit model are shown in Fig. 3. For $Z_{in} = Z_{out} = 50 \ \Omega$, the values of lamped components are as follows: $C_p = 19.97$ pF, $C_s = 8$ pF, $C_r = 30.7$ pF, $L_r = 0.228$ nH. The agreement between the HFSS simulation results and circuit model is obtained.
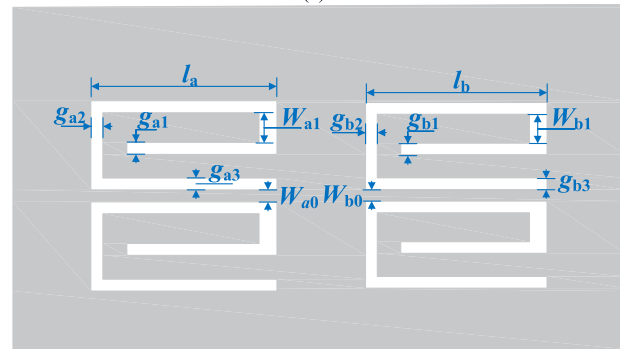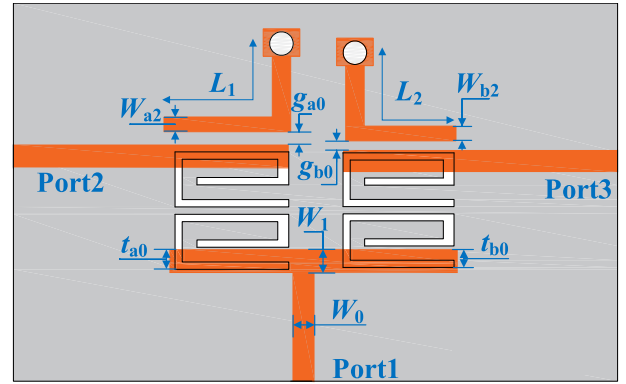

FIGURE 4. Configurations of the proposed SDGR diplexer: (a) microstrip feedlines and resonators at the top layer, and (b) etched helical type resonator on the ground.
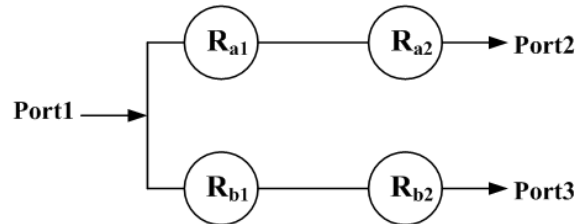

FIGURE 5. Coupling diagram of the SDGR diplexer.

B. DESIGN AND ANALYSIS OF THE COMPACT DIPLEXER

The proposed geometrical profile of the diplexer is shown in Fig. 4. Fig. 5 shows the coupling diagram. The diplexer consists of a common feed line and two separate filter channels with different size. Each channel contains a second-order Chebyshev band-pass filter with a ripple factor of 0.1. The second order low pass Chebyshev filter prototype value are $g_0 = 1$, $g_1 = 1.1468$, $g_2 = 1.3712$. The SDGR filters have central frequencies of 1.78 GHz with a 3 dB bandwidth of 9.6% and 2.4 GHz with a 3 dB bandwidth of 10.8%. The external quality factors and coupling coefficients, as referring to the proposed coupling diagram can be determined by [40]

$$Q_{e1} = \frac{g_0 g_1}{FBW} \tag{7}$$

$$Q_{en} = \frac{g_n g_{n+1}}{FBW} \tag{8}$$

$$k_{i,i+1} = \frac{FBW}{\sqrt{g_i g_{i+1}}}, \quad \text{for i} = 1 \text{ to } n-1 \tag{9}$$

where Q_{e1} and Q_{en} are the external quality factors of the resonators at the input and output ports, respectively, $k_{i,i+1}$ are the coupling coefficients between two adjacent resonators, g_{ns} indicate the element values of low-pass prototype filter, and n and FBW indicate the order and fractional bandwidth of the filter, respectively.

In the meantime, the two defected ground resonators, such as larger apertures, are designed for enhancing couplings as well. In order to obtain the dimensions of the two filters, full-wave simulator has been used to extract the external quality factors and coupling coefficients. The external quality factor can be obtained by

$$Q_e = \frac{f_0}{\Delta f_{\pm 90^0}} \qquad (10)$$

where f_0 and $\Delta f_{\pm 90^0}$ represent the resonant frequency and the bandwidth of $90°$ from central frequency, respectively. The final step is to individually adjust the coupling gaps between resonators to meet the desired coupling coefficients of Channel 1 and Channel 2 filters. When two synchronously tuned coupled resonators have a close proximity, the coupling coefficient can be evaluated from two dominant resonant frequencies. If f_1 and f_2 are defined as the lower and upper resonant frequencies, respectively, the coupling coefficient can be obtained by

$$k = \pm \frac{f_1^2 - f_2^2}{f_1^2 + f_2^2} \qquad (11)$$

Q_{ei} of the two channel filters (Q_{eiI} and Q_{eiII}) can be adjusted independently by changing the relative position between the resonator and the common feedline. The interaction between the two channels is very small, so the external quality factor of the two passbands can be achieved at the same time. The positional relationship between the resonator and the common feedline is adopted in order to acquire the desired external quality factor, as shown in Fig. 6. Fig. 6 (a) shows the simulated Q_{ei1} versus t_a. The resonator R_{b2} is introduced after t_a is determined based on the bandwidth of the diplexer so as to extract the relationship between the quality factor Q_{e2} of the channel 2 and the position t_b. According to Fig. 6(b), the change of Q_1 is very small when the position of the resonator R_{b1} is changed, so that once the bandwidth, order and ripple of the filter type are given, t_a and t_b can be determined respectively.

The initial values of the coupling coefficients between the resonators at different locations are extracted by the formula (11). As shown in Fig. 7, the coupling coefficients of the two adjacent resonators are given respectively. It can be seen that the larger the spacing between the resonators is, the smaller the coupling coefficient is. The initial values of W_{a0} and W_{b0} are 0.2 mm and 0.15 mm, respectively.

In order to improve the frequency selection characteristics of the passband and the isolation between the passbands, the quarter-wavelength resonators are connected in parallel to the two output ports. A transmission zero occurs at 2.4 GHz in the first passband, and a transmission zero is generated
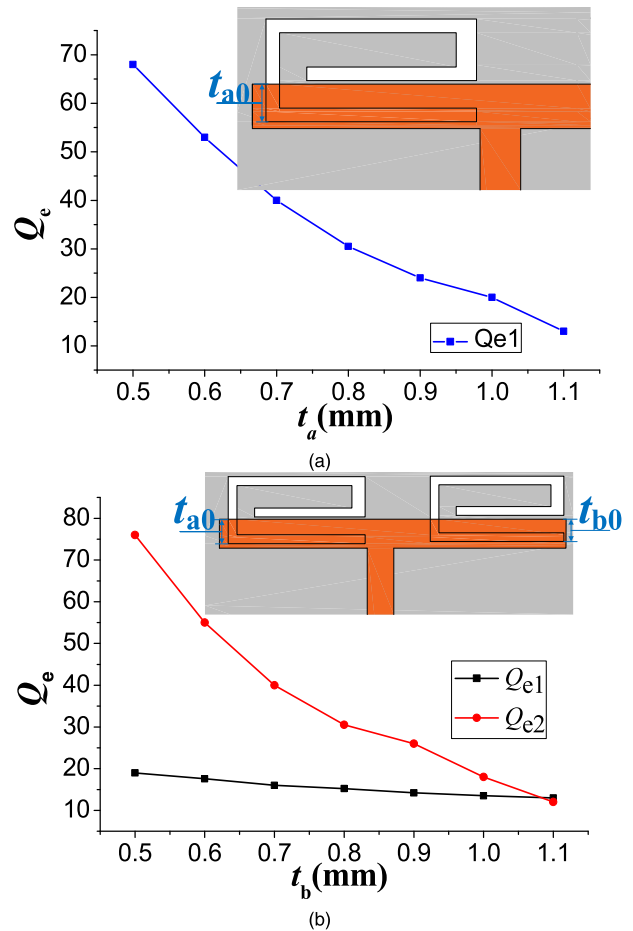

(a)

(b)

FIGURE 6. Extraction of external quality factors. (a) Simulated Q_{ei1} versus t_a (with w = 1.2mm). (b) Simulated Q_{ei2} versus t_b (with w = 1.2mm and t_a = 1.1mm).

at 1.8 GHz in the second passband. While the short-circuit resonator was folded, so the size of the entire circuit is still very small.

C. EXPERIMENT OF THE COMPACT DIPLEXER

Based on the above analysis, a diplexer is designed. The final size of the circuit is optimized by electromagnetic simulation software HFSS. The circuit is fabricated on an RF35 substrate with a dielectric constant of 3.5 and a thickness of 0.5 mm as shown in Fig. 8. As a final result, the viable design parameters of the diplexer are: $W_0 = W_1 = 1.11$ mm, $W_0 = 0.1$ mm, $W_{a1} = W_{a2} = 0.2$ mm, $g_{a0} = 0.1$ mm, $g_{a1} = g_{a2} = 0.2$ mm, $g_{a3} = 0.1$ mm, $t_{a1} = 1.1$ mm, $t_{a2} = 0.6$ mm, $l_a = 9.4$ mm, $s_{a1} = 9.5$ mm, $s_{a2} = 5.5$ mm, $W_{b1} = 0.15$ mm, $W_{b1} = 0.2$ mm, $g_{b1} = g_{b2} = 0.2$ mm, $g_{b3} = 0.1$ mm, $t_{b1} = 1$ mm, $t_{b2} = 0.58$ mm, $l_b = 6.8$ mm, $S_{b1} = 9.5$ mm, $S_{b2} = 6.4$ mm. The fabricated diplexer has a compact size of 14 mm×32 mm (0.14λ g× 0.31λ g, λ g is the wavelength of the first passband center frequency).

The diplexer is measured with an Agilent 8757D network analyzer. The simulated and measured results are illustrated in Fig. 9. The measured minimum insertion loss are 1.59 dB and 1.56 dB in the lower and upper passbands centered at
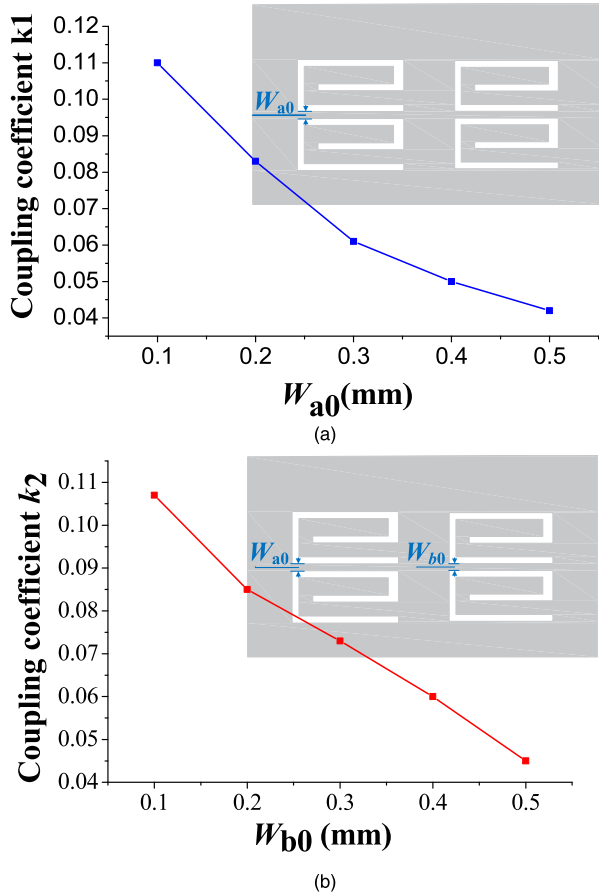
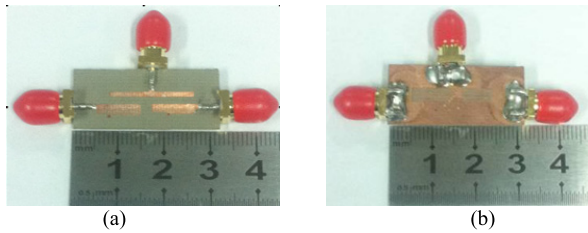FIGURE 7. (a) Simulated coupling coefficient k₁ versus w_a0. (b) Simulated k₂ versus w_b0.

FIGURE 8. Photograph of the fabricated SDGR diplexer: (a) top view (b) bottom view.

FIGURE 9. Simulated and measured results of the compact SDGR diplexer: (a) Insertion and return loss (b) isolation (c) out-of-band rejection.

1.8 GHz and 2.45 GHz with 3-dB fractional bandwidths of 9.5% and 10.7%, respectively. The isolations between the two channels are 40 dB and 46 dB at the center frequencies. In the operating frequency band from 1.8 GHz to 3.4 GHz, the isolation is all better than 30 dB. The wide stopband response is measured and is shown in Fig. 9(c). Due to the existence of slow wave effect in the defective structure, out-of-band suppression is greater than 10 dB in the 3-20 GHz frequency range, which means $11.1f_0$, while the stopband of circuits with the same performance is generally in no more than $3f_0$ [13], [20], [27]. The measure results are in good agreement with the simulation result. The increase in the measured insertion loss is mainly due to machining errors, and the error caused by the SMA connector. In Table 1, this
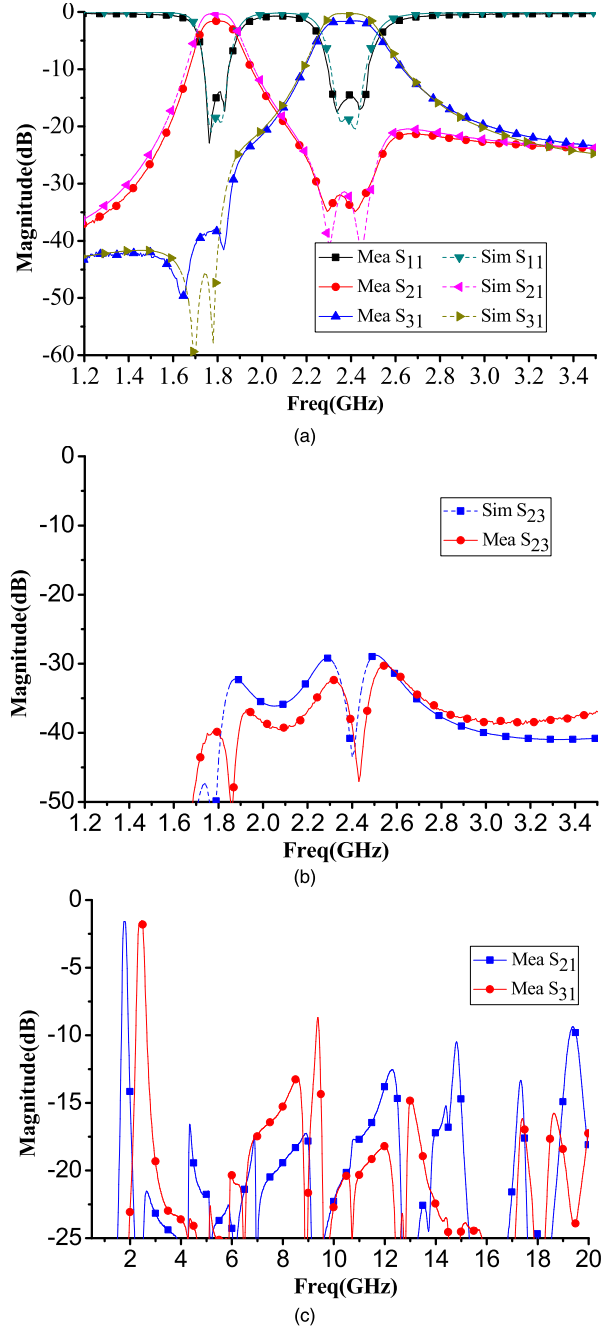
work is compared with other published work. It presents a more compact size and good performance.

III. STRUCTURE AND DESIGN OF THE TRIPLEXER

The proposed compact SDGR triplexer is shown in Fig. 10. Compared with above diplexer, a filter channel consisting of DSR is added to the common feedline. The center frequency of the added passband is 3.5 GHz and the relative bandwidth is 9.5%. The design process of the triplexer is as follows:

Firstly, based on the center frequency and frequency selectivity, the external quality factor and coupling coefficient

TABLE 1. Comparison with reported researches.

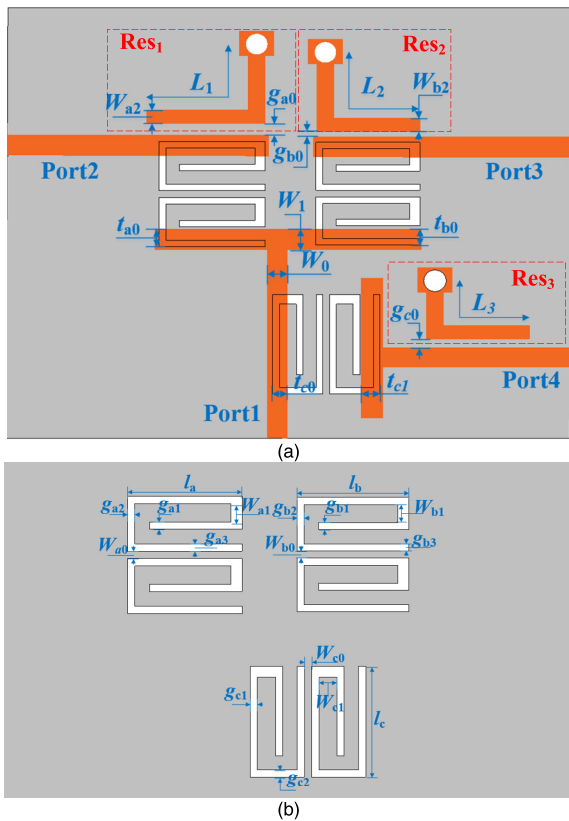|	f_0 (GHz)	IL (dB)	FBW (%)	Size ($\lambda_g \times \lambda_g$)	Iso (dB)	Stopband
[13]	1.95, 2.14	1.2, 1.5	4.1,3.3 4	0.36× 0.38	40, 35	
[20]	2.44, 3.52	1.43, 1.59	7.2,7.2	0.48× 0.58	42, 40	$2.2f_0$(-15dB)
[26]	1,1.2	2.22, 2.24	10,9	0.4× 0.55	37	$14.8f_0$(28dB)
[27]	2.7,2.8	2.7, 2.8	3.4,3.4	0.28× 0.44	45, 40	$1.6f_0$(-30dB)
This work	1.8, 2.45	1.59, 1.56	9.5, 10.7	0.14× 0.31	40, 46	$11.1f_0$(-10dB)

FIGURE 10. Configurations of the proposed compact SDGR diplexer: (a) microstrip feedlines and resonators at the top layer, and (b) etched helical type resonator on the ground.

TABLE 2. External quality factor and coupling coefficient of the triplexer.

Channels	f_0 (GHz)	FBW	Q_e	K_{12}
1	1.8	19.6%	12.087	0.076
2	2.4	10.8%	11.462	0.086
3	3.6	9.5%	12.072	0.076

are determined. As shown in Table 2, the external quality factor and the coupling coefficient are obtained according to Equ. (10) and (11). Thus, the dimensions of three parts of SDGR can be determined.

Secondly, the external quality factor Q_e and the coupling coefficient between adjacent resonators are extracted
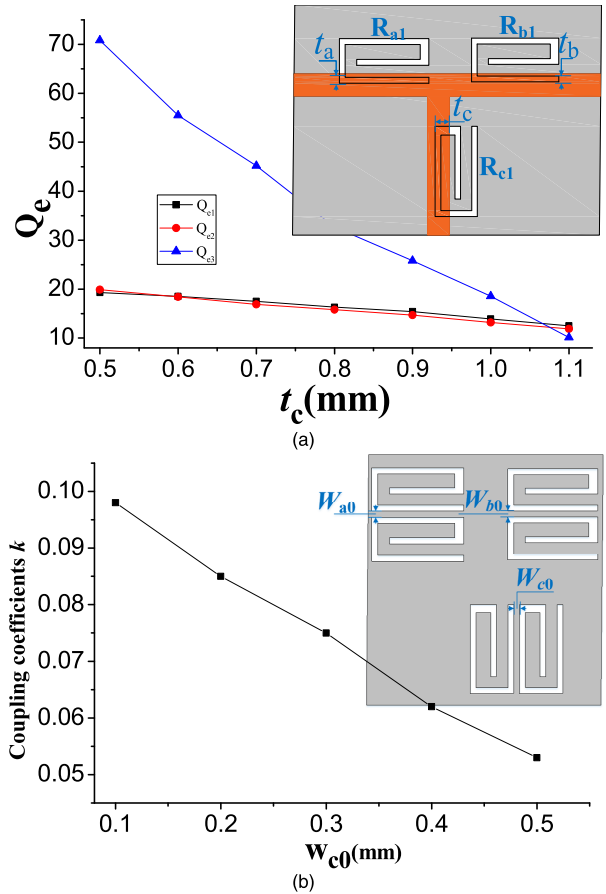

FIGURE 11. Extraction of (a) external quality factor and (b) coupling coefficient of the triplexer.
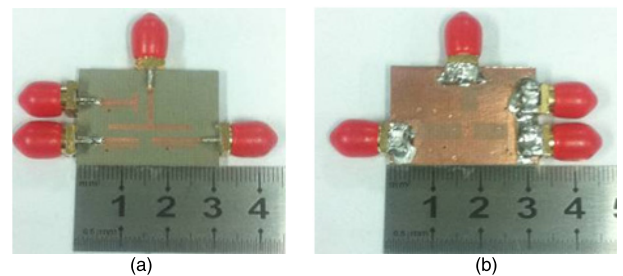

FIGURE 12. Photograph of the fabricated SDGR triplexer: (a) top view (b) bottom view.

by using the electromagnetic simulation software HFSS. As shown in Fig. 11 (a), when R_{a1}, R_{b1}, and the common feedline are determined, R_{c1} of the channel 3 is added. It can be seen that the larger the t_c is, the smaller the external quality factor Q_e is, which is consistent with the relationship between R_{a1}, R_{b1}, and the position of the common feedline.

In addition, the addition of the third part of resonator has little effect on the external quality factor of the other two passbands. The coupling coefficient is extracted by adjusting W_{c0}. The initial value W_{c0} can be obtained according to Fig. 11 (b).The central frequency and working bandwidth of the three passbands can be adjusted in dependently.
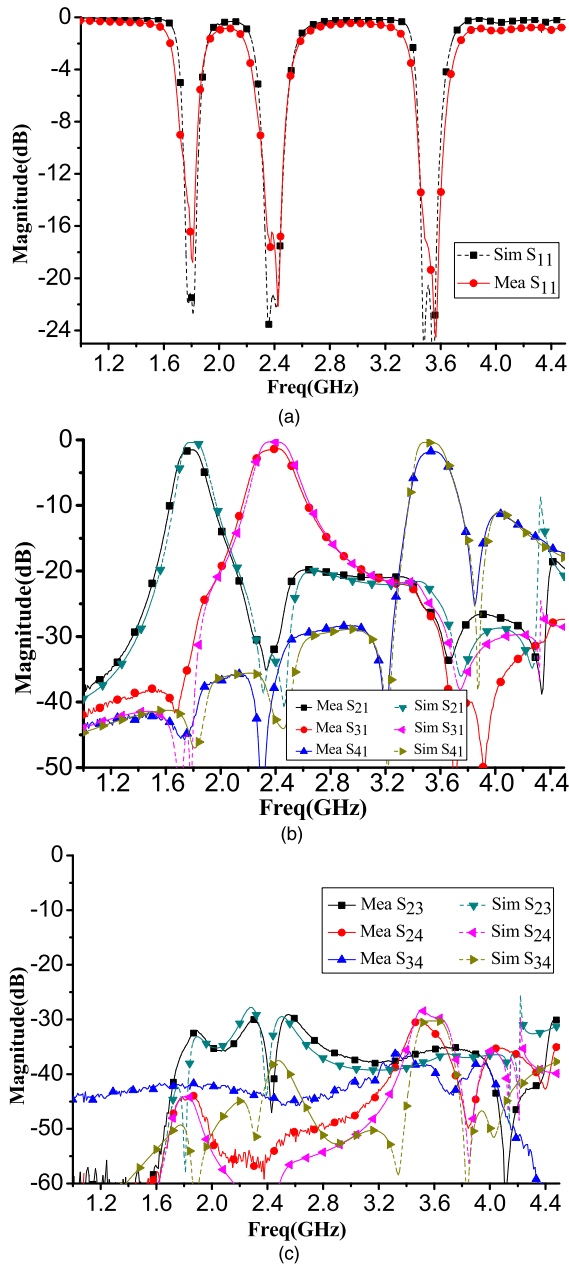
FIGURE 13. Simulated and measured results of the compact SDGR triplexer: (a) insertion and return loss (b) isolation (c) out-of-band rejection.

Finally, by optimizing the parameters, the triplexer is designed. In order to further improve the isolation between the channels, the quarter-wavelength short-circuit resonators are added. Comparison of transmission characteristics and isolation in band with or without quarter-wavelength resonators(Res1, Res2 and Res3) is shown in Fig. 12. A transmission zero is generated at 3.9GHz, increasing frequency selectivity and isolation between channels.

According to the design procedures presented above, the proposed compact diplexer is designed. This compact diplexer is fabricated and its photographs are shown in Fig. 13. The physical parameters of the third passband

are: $t_{c0} = 0.75$ mm, $t_{c1} = 0.6$ mm, $s_{c1} = 6.5$ mm, $s_{c2} = 0.2$ mm, $W_{c0} = 0.17$ mm, $W_{c1} = 0.2$ mm, $W_{c2} = 0.2$ mm, $g_{c0} = 0.1$ mm, $g_{c1} = 0.2$ mm, $g_{c2} = 0.2$ mm, $g_{c3} = 0.1$ mm, $l_c = 4.6$ mm. The overall size of the circuit is 20 mm×32 mm ($0.19\lambda g \times 0.31\lambda g$, λg is the waveguide wavelength of the first passband center frequency). Compared to the diplexer, the size of the triplexer do not increase significantly. The triplexer was measured using the Agilent 8757D's Vector Network Analyzer. The simulated and measured results are illustrated in Fig. 13. The measured center frequencies of Channels 1, 2, and 3 are 1.79 GHz, 2.4 GHz, and 3.54GHz with fractional bandwidths of 9.7%, 10.9%, and 9.7%, respectively. The minimum in-band insertion loss are 1.52 dB, 1.35 dB, and 1.76 dB, respectively. The isolation between three channels is greater than 30 dB. The measured results are in good agreement with the simulation ones.

IV. CONCLUSION
In this paper, a compact diplexer and triplexer with high isolation, and wide stopband have been designed. The miniature diplexer or triplexer consists of feedline and spiral defected ground resonator. The design process is relatively simple and easy to implement by using the defective structure to design the multiplexer. The introduction of the defective structure makes the influence of the pass band small, and each passband can be designed independently. On the other hand, due to the slow wave effect of the SDGR, a wider stopband characteristic is realized on the basis of miniaturization. Since the size of the multiplexer is very small, it is easy to form other bandpass responses by adding more SDGR cells without increasing too much extra size of the components. Finally, the proposed diplexer and triplexer are fabricated and measured. Measurements of this kind fabricated multiplexer match the simulations well.

REFERENCES
[1] J. Xu, W. Wu, and C. Miao, "Compact microstrip dual-/tri-/quad-band bandpass filter using open stubs loaded shorted stepped-impedance resonator," *IEEE Trans. Microw. Theory Techn.*, vol. 61, no. 9, pp. 3187–3199, Sep. 2013.

[2] P. C. Loh, L. Zhang, and F. Gao, "Compact integrated energy systems for distributed generation," *IEEE Trans. Ind. Electron.*, vol. 60, no. 4, pp. 1492–1502, Apr. 2013.

[3] J. Xu and Y. Zhu, "Tunable bandpass filter using a switched tunable diplexer technique," *IEEE Trans. Ind. Electron.*, vol. 64, no. 4, pp. 3118–3126, Apr. 2017.

[4] X. Q. Lin, J. Y. Jin, J. W. Yu, Y. Jiang, Y. Fan, and Q. Xue, "Design and analysis of EMIT filter and diplexer," *IEEE Trans. Ind. Electron.*, vol. 64, no. 4, pp. 3059–3066, Apr. 2017.

[5] K. Song and Q. Xue, "Ultra-wideband ring-cavity multiple-way parallel power divider," *IEEE Trans. Ind. Electron.*, vol. 60, no. 10, pp. 4737–4745, Oct. 2013.

[6] K. Song, F. Zhang, S. Hu, and Y. Fan, "Ku-band 200-W pulsed power amplifier based on waveguide spatially power-combining technique for industrial applications," *IEEE Trans. Ind. Electron.*, vol. 61, no. 8, pp. 4274–4280, Aug. 2014.

[7] B. H. Choi, V. X. Thai, E. S. Lee, J. H. Kim, and C. T. Rim, "Dipole-coil-based wide-range inductive power transfer systems for wireless sensors," *IEEE Trans. Ind. Electron.*, vol. 63, no. 5, pp. 3158–3167, May 2016.

[8] Z. Wang, J. Hu, J. Han, G. Zhao, J. He, and S. X. Wang, "A novel high-performance energy harvester based on nonlinear resonance for scavenging power-frequency magnetic energy," *IEEE Trans. Ind. Electron.*, vol. 64, no. 8, pp. 6556–6564, Aug. 2017.

[9] G.-L. Huang, S.-G. Zhou, and T.-H. Chio, "Highly-efficient self-compact monopulse antenna system with integrated comparator network for RF industrial applications," *IEEE Trans. Ind. Electron.*, vol. 64, no. 1, pp. 674–681, Jan. 2017.

[10] H. Li, X. Zhao, W. Su, K. Sun, X. You, and T. Q. Zheng, "Nonsegmented PSpice circuit model of GaN HEMT with simulation convergence consideration," *IEEE Trans. Ind. Electron.*, vol. 64, no. 11, pp. 8992–9000, Nov. 2017.

[11] N. Damavandi and S. Safavi-Naeini, "A hybrid evolutionary programming method for circuit optimization," *IEEE Trans. Circuits Syst. I, Reg. Papers*, vol. 52, no. 5, pp. 902–910, May 2005.

[12] M. Karlsson, A. Serban, J. Osth, Owais, and S. Gong, "Frequency triplexer for ultra-wideband systems (6–9 GHz)," *IEEE Trans. Circuits Syst. I, Reg. Papers*, vol. 60, no. 3, pp. 540–547, Mar. 2013.

[13] X. Guan, F. Yang, H. Liu, and L. Zhu, "Compact and high-isolation diplexer using dual-mode stub-loaded resonators," *IEEE Microw. Wireless Compon. Lett.*, vol. 24, no. 6, pp. 385–387, Jun. 2014.

[14] D. Bukuru, K. Song, F. Zhang, Y. Zhu, and M. Fan, "Compact quad-band bandpass filter using quad-mode stepped impedance resonator and multiple coupling circuits," *IEEE Trans. Microw. Theory Techn.*, vol. 65, no. 3, pp. 783–791, Mar. 2017.

[15] Q. Xu, "Design and development of a compact flexure-based XY precision positioning system with centimeter range," *IEEE Trans. Ind. Electron.*, vol. 61, no. 2, pp. 893–903, Feb. 2014.

[16] M. Bekheit, S. Amari, and W. Menzel, "Modeling and optimization of compact microwave bandpass filters," *IEEE Trans. Microw. Theory Techn.*, vol. 56, no. 2, pp. 420–430, Feb. 2008.

[17] X. Guan *et al.*, "Compact, low insertion-loss, and wide stopband HTS diplexer using novel coupling diagram and dissimilar spiral resonators," *IEEE Trans. Microw. Theory Techn.*, vol. 64, no. 8, pp. 2581–2589, Aug. 2016.

[18] K. Song, Y. Mo, Q. Xue, and Y. Fan, "Wideband four-way out-of-phase slotline power dividers," *IEEE Trans. Ind. Electron.*, vol. 61, no. 7, pp. 3598–3606, Jul. 2014.

[19] M.-L. Chuang and M.-T. Wu, "Microstrip diplexer design using common T-shaped resonator," *IEEE Microw. Wireless Compon. Lett.*, vol. 21, no. 11, pp. 583–585, Nov. 2011.

[20] J.-K. Xiao, M. Zhu, Y. Li, L. Tian, and J.-G. Ma, "High selective microstrip bandpass filter and diplexer with mixed electromagnetic coupling," *IEEE Microw. Wireless Compon. Lett.*, vol. 25, no. 12, pp. 781–783, Dec. 2015.

[21] J.-T. Kuo and E. Shih, "Microstrip stepped impedance resonator bandpass filter with an extended optimal rejection bandwidth," *IEEE Trans. Microw. Theory Techn.*, vol. 51, no. 5, pp. 1554–1559, May 2003.

[22] J.-S. Hong and S. Li, "Theory and experiment of dual-mode microstrip triangular patch resonators and filters," *IEEE Trans. Microw. Theory Techn.*, vol. 52, no. 4, pp. 1237–1243, Apr. 2004.

[23] C. Karpuz, A. K. Gorur, and M. Emur, "Quad-band microstrip bandstop filter design using dual-mode open loop resonators having thin film capacitors," *IEEE Microw. Wireless Compon. Lett.*, vol. 26, no. 11, pp. 873–875, Nov. 2016.

[24] J.-S. Hong, H. Shaman, and Y.-H. Chun, "Dual-mode microstrip open-loop resonators and filters," *IEEE Trans. Microw. Theory Techn.*, vol. 55, no. 8, pp. 1764–1770, Aug. 2007.

[25] L. Athukorala and D. Budimir, "Compact dual-mode open loop microstrip resonators and filters," *IEEE Microw. Wireless Compon. Lett.*, vol. 19, no. 11, pp. 698–700, Nov. 2009.

[26] F.-C. Chen *et al.*, "Design of wide-stopband bandpass filter and diplexer using uniform impedance resonators," *IEEE Trans. Microw. Theory Techn.*, vol. 64, no. 12, pp. 4192–4203, Dec. 2016.

[27] C.-F. Chen, T.-Y. Huang, C.-P. Chou, and R.-B. Wu, "Microstrip diplexers design with common resonator sections for compact size, but high isolation," *IEEE Trans. Microw. Theory Techn.*, vol. 54, no. 5, pp. 1945–1952, May 2006.

[28] S. Tantiviwat, N. Intarawiset, and R. Jeenawong, "Wide-stopband, compact microstrip diplexer with common resonator using stepped-impedance resonators," in *Proc. IEEE Tencon-Spring*, Apr. 2013, pp. 174–177.

[29] K. Zhou, C.-X. Zhou, and W. Wu, "Resonance characteristics of substrate-integrated rectangular cavity and their applications to dual-band and wide-stopband bandpass filters design," *IEEE Trans. Microw. Theory Techn.*, vol. 65, no. 5, pp. 1511–1524, May 2017.

[30] C.-F. Chen, T.-M. Shen, T.-Y. Huang, and R.-B. Wu, "Design of multimode net-type resonators and their applications to filters and multiplexers," *IEEE Trans. Microw. Theory Techn.*, vol. 59, no. 4, pp. 848–856, Apr. 2011.

[31] C.-S. Kim, J.-S. Park, D. Ahn, and J.-B. Lim, "A novel 1-D periodic defected ground structure for planar circuits," *IEEE Microw. Guided Wave Lett.*, vol. 10, no. 4, pp. 131–133, Apr. 2000.

[32] D. Ahn, J.-S. Park, C.-S. Kim, J. Kim, Y. Qian, and T. Itoh, "A design of the low-pass filter using the novel microstrip defected ground structure," *IEEE Trans. Microw. Theory Techn.*, vol. 49, no. 1, pp. 86–93, Jan. 2001.

[33] J.-S. Lim, H.-S. Kim, J.-S. Park, D. Ahn, and S. Nam, "A power amplifier with efficiency improved using defected ground structure," *IEEE Microw. Wireless Compon. Lett.*, vol. 11, no. 4, pp. 170–172, Apr. 2001.

[34] F.-C. Chen, H.-T. Hu, J.-M. Qiu, and Q.-X. Chu, "High-selectivity low-pass filters with ultrawide stopband based on defected ground structures," *IEEE Trans. Compon., Packag., Manuf. Technol.*, vol. 5, no. 9, pp. 1313–1319, Sep. 2015.

[35] H.-J. Chen *et al.*, "A compact bandpass filter with enhanced stopband characteristics by an asymmetric cross-shape defected ground structure," *IEEE Trans. Ultrason., Ferroelectr., Freq. Control*, vol. 53, no. 11, pp. 2183–2187, Nov. 2006.

[36] J. Z. Chen, N. Wang, K. Deng, and S. Yang, "Design of compact quadruplexer based on defected stepped impedance resonators," *Prog. Electromagn. Res.*, vol. 119, no. 2, pp. 19–33, 2011.

[37] J.-S. Lim, C.-S. Kim, Y.-T. Lee, D. Ahn, and S. Nam, "A spiral-shaped defected ground structure for coplanar waveguide," *IEEE Microw. Wireless Compon. Lett.*, vol. 12, no. 9, pp. 330–332, Sep. 2002.

[38] J.-S. Lim, C.-S. Kim, Y.-C. Jeong, D. Ahn, and S. Nam, "An advanced equivalent circuit of spiral-shaped defected ground structure," in *Proc. 34th Eur. Microw. Conf.*, Oct. 2004, pp. 1357–1360.

[39] M. Zhou, C.-M. Tong, S.-H. Fu, L.-N. Wu, and X.-M. Li, "A novel spiral defected ground structure and its application to the design of dual bandstop filter," in *Proc. Int. Symp. Signals, Syst. Electron.*, Sep. 2010, pp. 1–3.

[40] J.-S. Hong and M. J. Lancaster, "Coupled resonator circuits," in *Microstrip Filters for RF / Microwave Applications*. Hoboken, NJ, USA: Wiley, 2001, pp. 235–272.

KAIJUN SONG (M'09–SM'12) received the M.S. degree in radio physics and the Ph.D. degree in electromagnetic field and microwave technology from the University of Electronic Science and Technology of China (UESTC), Chengdu, China, in 2005 and 2007, respectively.

From 2007 to 2008, he was a Postdoctoral Research Fellow with Montana Tech, University of Montana, Butte, USA, where he was involved in microwave/millimeter-wave circuits and microwave remote sensing technologies. From 2008 to 2010, he was a Research Fellow with the State Key Laboratory of Millimeter Waves of China, Department of Electronic Engineering, City University of Hong Kong, where he was involved in microwave/millimeter-wave power-combining technology and ultra-wideband (UWB) circuits. He was a Senior Visiting Scholar with the State Key Laboratory of Millimeter Waves of China, Department of Electronic Engineering, City University of Hong Kong, in 2012. He was a Full Professor with UESTC, where he has been with the EHF Key Laboratory of Science, School of Electronic Engineering, since 2007. Since 2018, he has been a Full Professor with the School of Electronic Science and Engineering, UESTC. He has published more than 200 internationally refereed journal papers and conference papers. His current research interests include microwave and millimeter-wave/ THz power-combining technology, UWB circuits and technologies, microwave/millimeter-wave devices, circuits, and systems, and microwave remote sensing technologies. In 2011, he received the New Century Excellent Talents in University Award from the Chinese Ministry of Education. In 2015, he received the Academic and Technical Leaders in Sichuan Province Award. He is a Reviewer for tens of international journals, including the IEEE TRANSACTIONS and IEEE LETTERS.
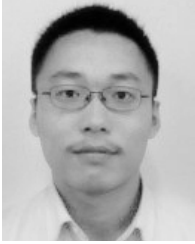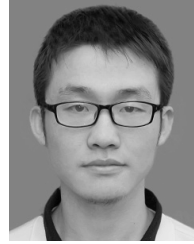
YEDI ZHOU was born in Harbin, Heilongjiang, China, in 1991. He received the B.S. degree from the University of Electronic Science and Technology of China, Chengdu, China, in 2013, where he is currently pursuing the Ph.D. degree in electromagnetic fields and microwave technology. His research interests include microwave- and millimetre-wave power-combining technology.
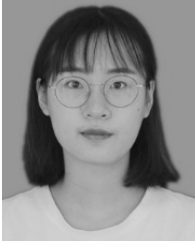
YUXUAN CHEN was born in Nanchang, Jiangxi, China, in 1996. She received the B.S. degree in engineering from Southwest University, Chongqing, China, in 2018. She is currently pursuing the M.S. degree in electronics and communication engineering with the University of Electronic Science and Technology of China. Her research interests include millimetre-wave and terahertz-wave power-combining technology.

SHEMA RICHARD PATIENCE was born in Kigali, Rwanda, in 1988. He received the B.Sc. degree in electrical and electronic engineering from the National University of Rwanda, Huye, Rwanda, in 2012, and the M.Eng. degree in electronic science and technology from the Beijing Institute of Technology, Beijing, China, in 2015. He is currently pursuing the Ph.D. degree with the University of Electronic Science and Technology of China. His research interests include microwave/millimeter wave substrate-integrated waveguide power dividers/combiners and passive components design in RF circuits.

SONG GUO was born in Langfang, Hebei, China, in 1993. He received the B.Sc. degree in microelectronics from Harbin Engineering University, Harbin, Heilongjiang, China, in 2006. He is currently pursuing the Ph.D. degree in electromagnetic fields and microwave technology with the University of Electronic Science and Technology of China. His research interests include microwave- and millimetre-wave power-combining technology and microwave passive component design.

YONG FAN (M'05–SM'18) received the B.E. degree from the Nanjing University of Science and Technology, Nanjing, Jiangsu, China, in 1985, and the M.S. degree from the University of Electronic Science and Technology of China, Chengdu, Sichuan, China, in 1992.

He has authored or co-authored over 100 papers, 80 of which are searched by SCI and EI. From 1985 to 1989, he was interested in microwave integrated circuits. Since 1989, his research interests include millimeter-wave communication, electromagnetic theory, millimeter-wave technology, and millimeter-wave systems. He is a Senior Member of the Chinese Institute of Electronics.

● ● ●